

Discontinuous Galerkin Method for Investigating Ice Strength

V. A. Miryaha^{a, b, *}, A. V. Sannikov^b, V. A. Biryukov^b, and I. B. Petrov^b

^a*Keldysh Institute of Applied Mathematics, Russian Academy of Sciences, Moscow, 125047 Russia*

^b*Moscow Institute of Physics and Technology, Moscow, 117303 Russia*

**e-mail: vlad.miryaha@gmail.com*

Received May 15, 2017

Abstract—This paper discusses the numerical modeling of various ice-strength measurement experiments, including uniaxial compression and bending, and it also compares the data obtained by field and numerical experiments. Numerical simulation is based on a dynamic system of continuum mechanics equations with ice considered as an elasto-plastic medium with brittle and crushing fracture dynamic criteria. The simulation software developed by the authors is based on the discontinuous Galerkin method and runs on high-performance systems with a distributed memory. Estimating the explicit values used by the mathematical models poses a major problem because some of them cannot be directly measured in field experiments due to the multiple interferences of physical processes. In practice, it is only possible to directly measure their total influence. However, this problem can be solved by comparing the numerical experiment with the field data. As a result of this work, the elasto-plastic ice model is verified and some missing physical properties are obtained by the numerical experiments.

Keywords: numerical simulation, discontinuous Galerkin method, elasto-plastic medium, and ice strength

DOI: 10.1134/S2070048218050083

1. INTRODUCTION

To determine the global and local ice loads on the structures of the continental shelf, semiempirical formulas from regulatory documents [1, 2], which include the uniaxial compression strength of ice as a factor, can be used. In turn, continuum mechanics models are usually more complex and involve a larger number of constants that describe the mechanical properties of ice. These constants determine the behavior of an infinitesimal volume of the medium. However, uniaxial compression strength, which is understood as the strength of a material, is fundamentally a macroscopic parameter that generally depends not only on the structure and physical state of ice but also on the shape and dimensions of a test sample. This also applies to the bending strength of ice (bending crushes ice due to excess tensile stress). Not all constitutive parameters of such models can be measured directly. In some works [3–5], similar mechanical and mathematical models were used and ice parameters were listed, but their original source and method of evaluation were not specified. Ice parameters depend on many factors, including temperature, salinity, and the deformation rate. A major problem is to find all the parameters for a mechanical-mathematical model of ice when working with an individual sample because typical experiments often imply its destruction. In other words, it is impossible to measure the bending and tensile strengths of the same sample. Moreover, the parameters of other samples may differ significantly due to the differences in the shape and height of ice under natural conditions.

The purpose of this work is to analyze the adequacy of the proposed mechanical-mathematical model of ice and to develop a method for finding model parameters in comparison to the data of an individual field experiment.

The paper is organized as follows. Sections 2 and 3 briefly describe the ice model and the numerical method used. Sections 4 and 5 present the results of the numerical experiments aimed at investigating the uniaxial compression strength and the four-point bending strength of ice. In Conclusions, we assess the experimental results and discuss the directions for further research.

2. MECHANICAL-MATHEMATICAL MODEL OF ICE

Ice has a complex structure and requires complex mechanical-mathematical models to describe its behavior. Some effects are difficult to take into account explicitly, because this significantly complicates the mechanical-mathematical model and also requires knowledge of additional constants, including special field experiments for their measurement and investigation. In this work, we use an elasto-plastic model of ice. The basic idea of the mechanical-mathematical model is consistent with the current trends in ice modeling [3–7]. Different authors make small modifications based on the experimental data, e.g., complicating the pressure dependence of the yield strength; however, these changes are not fundamental. In this work, we employ the Prandtl–Reis model with the Mises–Schleicher yield condition [8]. The system of constitutive equations can be written as follows:

$$\begin{cases} \rho \dot{v}_i = \nabla_j \sigma_{ij}, \\ \sigma_{ij} = q_{ijkl} \varepsilon_{kl}, \end{cases} \quad (1)$$

where

$$\begin{aligned} q_{ijkl} &= \lambda \delta_{ij} \delta_{kl} + \mu (\delta_{ik} \delta_{jl} + \delta_{il} \delta_{jk}) - \mu I \sigma_{ij} \sigma_{kl} / k^2, \\ k &= k_0 + \alpha p, \end{aligned} \quad (2)$$

$$I = \begin{cases} 0, & s_{ij} : s_{ij} < 2k^2, \\ 1, & s_{ij} : s_{ij} \geq 2k^2, \end{cases} \quad (3)$$

v_i are the components of the medium's velocity at a given point, σ_{ij} are the components of the Cauchy stress tensor, ε_{ij} are the components of the deformation tensor, ρ is density, λ and μ are the Lamé parameters, and k_0 and α are the material parameters that determine the instant of plastic flow or brittleness, while the stress deviator s_{ij} and pressure p are found by the formulas

$$s_{ij} = \sigma_{ij} + p \delta_{ij}, \quad p = -\frac{1}{3} \sigma_{ij}.$$

Conditions (2) and (3) are called the Mises–Schleicher conditions.

As failure criteria, we use the maximum principal stress and maximum plastic deformation. The maximum principal stress criterion suggests that if the maximum principal value of the stress tensor exceeds a certain threshold σ_{\max} , then ice cracks. The crack formation process is described as a replacement of the contact edge by two free boundaries. The maximum plastic deformation criterion implies that ice cracks when $\varepsilon_p = \sqrt{(2/3) \varepsilon_{ij}^p \varepsilon_{ij}^p}$ exceeds a certain value ε_p^{\max} . Here, $\varepsilon_{ij}^p = \int_0^t \dot{\varepsilon}_{ij} I dt$ is a plastic part of the deformation tensor, where

$$\dot{\varepsilon}_{ij} = \frac{1}{2} \left(\frac{dv_i}{dx_j} + \frac{dv_j}{dx_i} \right).$$

Since, after cracking, ice should be described as a fractured material (rather than as an elasto-plastic one), the mechanical parameters of the model in the area of cracking need to be adjusted. In this paper, we consider two variants of this adjustment. The first variant implies adjusting the second Lamé parameter on the condition of preserving the uniform compression coefficient:

$$\mu' = \alpha_\mu \mu.$$

In the case of stretching, the principal stresses are assumed to be zero. The second variant implies adjusting only the yield strength

$$k' = \alpha_k k.$$

Here, α_μ and α_k are assumed to be 0.1. As the initial ice parameters, we use those from [9] (see Table 1).

3. NUMERICAL METHOD

The system of constitutive Eqs. (1) is solved numerically by the discontinuous Galerkin method [10, 11]. The method is implemented as a software complex for 2D and 3D simulation, which is parallelized to run on computing systems with shared or distributed memory.

Table 1. Physical and mechanical characteristics of ice

Parameter	Value
Density, ρ , kg/m ³	910.0
Young's modulus, E , Pa	5.0×10^9
Shear modulus, G , Pa	1.87×10^9
Yield strength, k , Pa	2.2×10^6
Ultimate tensile strength, σ_{\max} , Pa	1.1×10^6
Fracture strain, ϵ_{\max}^p , %	1.0

4. UNIAXIAL COMPRESSION STRENGTH

Some parameters of the continuum mechanics model, which describes the strength characteristics of ice, are difficult to obtain directly from field experiments. However, having conducted a numerical experiment, they can be related with measurable macroscopic parameters. The uniaxial compression strength of ice is one of these macroscopic parameters, which, in fact, depends on microscopic parameters such as yield strength, ultimate tensile strength, and fracture strain. For the numerical simulation of the uniaxial compression measurement experiment, we select a setting whereby an ice cube is compressed with a constant speed of the press plate to analyze the dependence of the applied load on the axial displacement, as well as the fracture behavior of the sample. As the initial physical and mechanical parameters of ice, we use the data from Table 1. The ice sample is a cube with 15-cm sides whose faces are parallel to the press plates and are compressed at a constant speed of 10 cm/s. This problem is solved both in 2D and 3D statements: in the 2D statement, it is easier to compare fracture patterns; in the 3D statement, it is easier to compare the numerical values of the overall loads.

As a result of simulation, we obtain the fracture patterns shown in Fig. 1.

The external fracture pattern is clear enough and easily amenable to qualitative comparison with the field experiment; however, the internal fracture pattern is quite complex (Fig. 2 shows it in section).

The fracture pattern can be qualitatively compared with the results of the field experiments conducted under similar conditions (see Fig. 3). We carried out these experiments in the school seminar "Ice mechanics 2016" held at the Engineering School of the Far Eastern Federal University.

It should be noted that, despite the significantly different fracture patterns in field experiments, even under seemingly similar initial conditions, they exhibit common features that are qualitatively consistent with the nature of cracks in numerical experiments:

- vertical cracks formed as a result of local stretching dominate on the outside;
- the cone-shaped areas that are in direct contact with the press are the least exposed to fracturing;
- inside the sample, bulk fracturing dominates, which causes ice to crumble into fine crumbs.

The last two observations are obvious from the cylindrical samples in the field experiments (see Fig. 4).

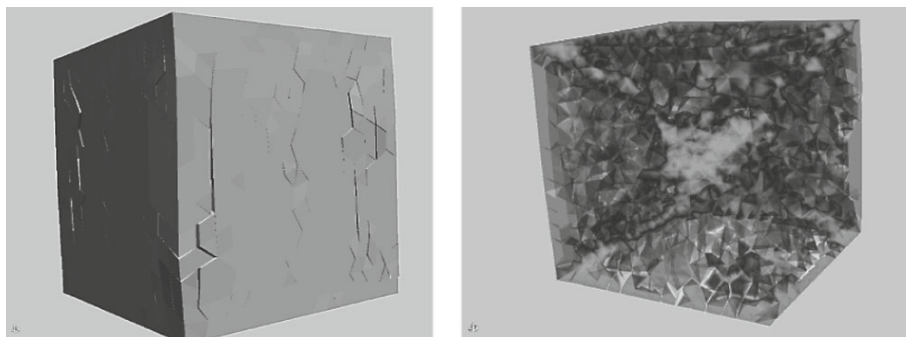


Fig. 1. External and internal fracture patterns of ice sample; internal fracture pattern demonstrates destruction by tensile criterion and bulk fracturing of cells.

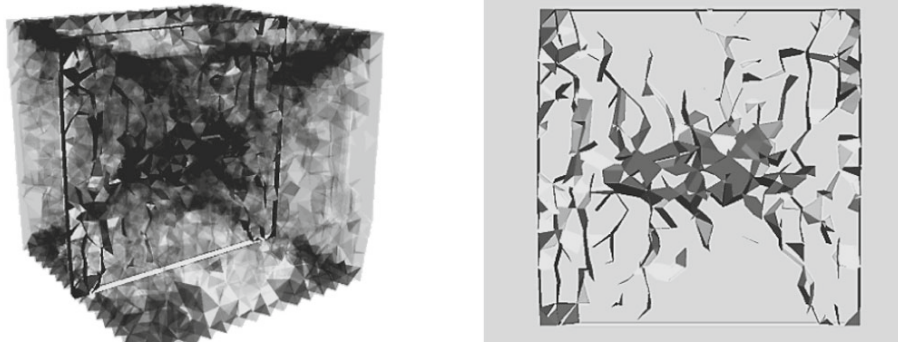


Fig. 2. Cross section of fracture pattern for ice sample.

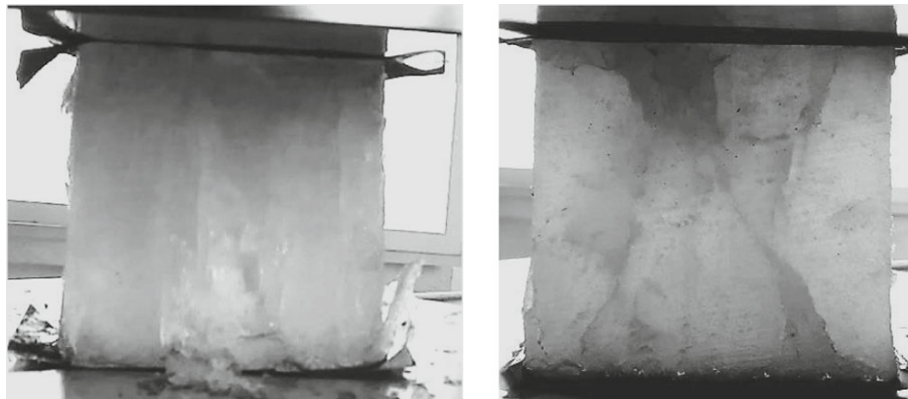


Fig. 3. Fracture patterns of ice sample in field experiments.

We also investigated the effect of the model parameters (yield strength k and fracture strain ϵ_{\max}^p) on the time dependence of the compression force acting on the sample (see Fig. 5). Curve 1 represents the compression force for the material parameters shown in Table 1. Curve 2 is constructed for $\epsilon_{\max}^p = 0$ (brittle ice), while curve 3 is obtained by a 25% reduction in yield strength k (as the temperature increases, ice becomes more plastic). In the section devoted to the mechanical-mathematical model, two possible variants of the parameter adjustment for the maximum plastic deformation criterion have been discussed. For curve 1, we use the first variant with the adjustment of the second Lamé parameter under condition of

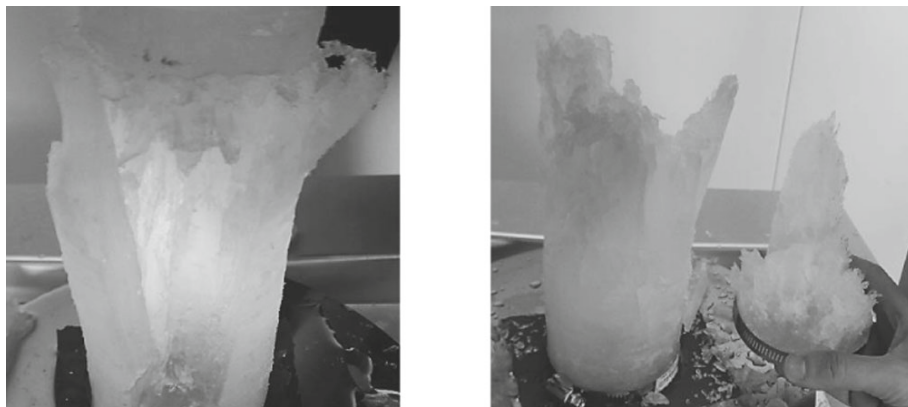


Fig. 4. Fracture patterns of cylindrical samples in field experiments (clamps at ends correspond to fixed boundary model).

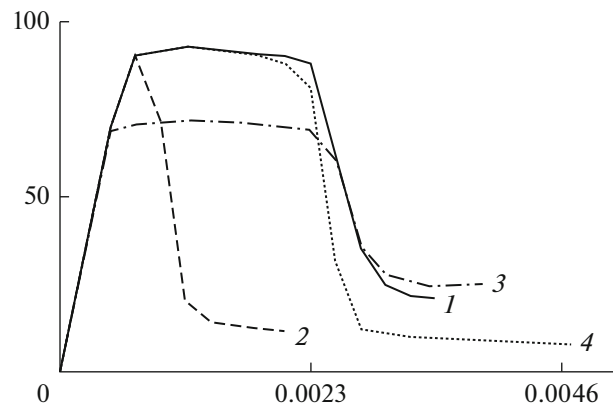


Fig. 5. Time dependences (s) of compression force (kN) plotted along y -axis when varying yield strength k and fracture strain ε_{\max}^p .

preserving the uniform compression coefficient; for curve 4, we use the second variant that implies adjusting only the yield strength while preserving the other model parameters.

This series of computations allows us to relate the macroscopic parameters of pressure and stress with the microscopic parameters of ice strength. For example, for curve 1 (see Fig. 5), the maximum compression strength of the sample is determined by the yield strength of ice; i.e., the bulk fracture criterion comes into action, with the ratio between the peak pressure at compression and the yield strength being

$$\frac{F_{\max}}{Sk} = \frac{9.2 \times 10^4 \text{ [N]}}{0.15^2 \text{ [m}^2\text{]} \times 2.2 \times 10^6 \text{ [Pa]}} \approx 1.86,$$

which is consistent with the value of 1.92 obtained in [8].

Figure 6 shows some fracture patterns for different values of the maximum plastic deformation parameter. Qualitative comparison of the fracture patterns in the field and numerical experiments allows us, by varying the parameters, to refine their values.

5. ICE BENDING STRENGTH

An experiment with four-point bending is quite suitable for investigating the tensile strength of ice. The geometry of the experiment (see Fig. 7) corresponds to the statement [10]; as the strength parameters, we use the parameters from Table 1 with the deformation rate being 5 cm/s for each side of the ice block. In the numerical experiment, we investigated the time dependence of the total load on one of the block's faces. Since the loading elements in the field experiment have a finite size, the forces of contact interaction are distributed over finite-width areas. The total load on the sample is computed as an integral of the corresponding components of the stress tensor with respect to the two upper or two lower contact areas. In the general case, integration over the contact areas can be replaced by integration over the entire face because the integral over the free noncontact surface does not contribute to the result.

Figure 8 shows the time dependence of the pressure force acting on the ice block. Up to the moment of fracturing, which occurs at ~ 0.1 s, tensile stresses at the top of the block increase up to a critical value

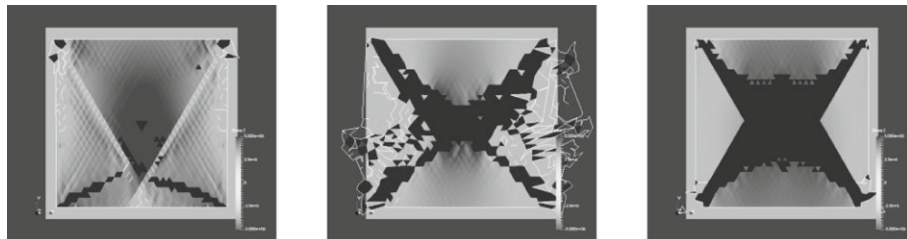


Fig. 6. Change in qualitative fracture pattern when varying maximum plastic deformation parameter (central computation corresponds to typical value, left limit is increased, while right limit is decreased).

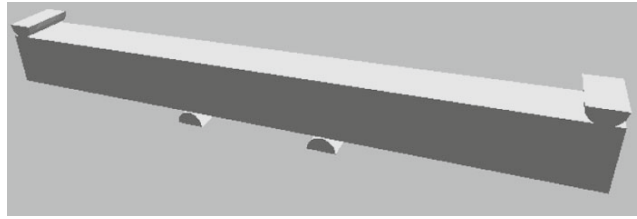


Fig. 7. Geometry of numerical experiment with four-point bending.

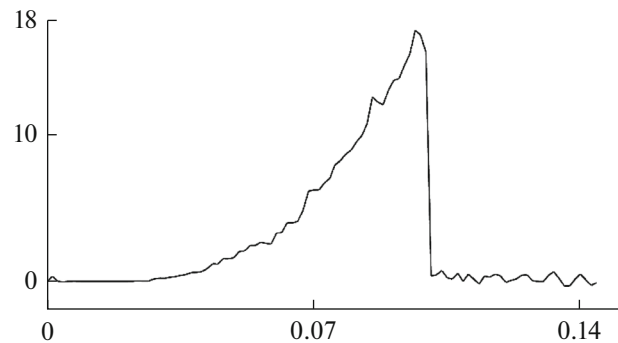


Fig. 8. Time dependence (s) of pressure (kN) on upper face of block, plotted along y-axis.

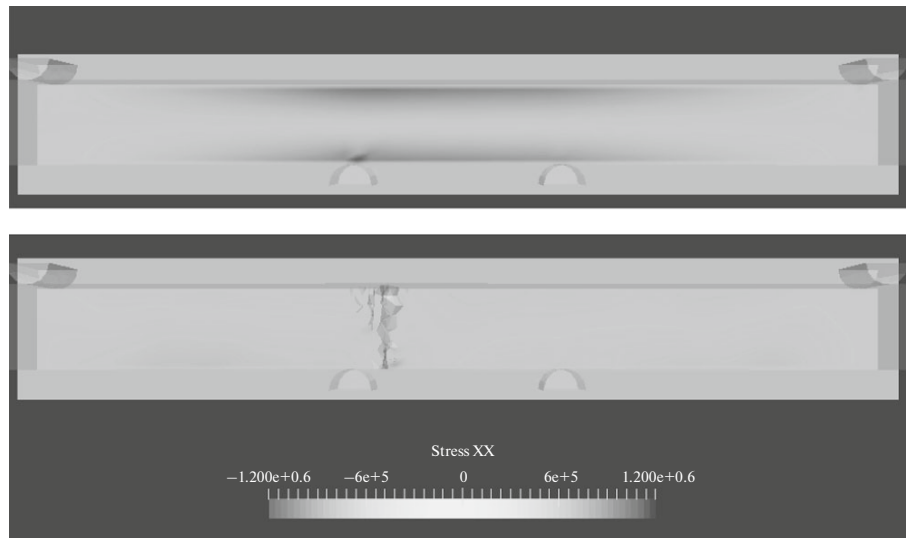


Fig. 9. Tensile stresses before and after formation of tensile crack.

equal to the ultimate tensile strength of ice, and then sharply decrease after the formation of a crack (see Figs. 9, 10). This allows the measured macroscopic parameters of the total force and displacement to be related with the microscopic parameter of tensile strength. In this computational experiment, we obtained a 17-kN peak load for a 1.1-MPa tensile strength, which agrees well (within an accuracy level of 10%) with the average peak load of 6.9 kN for a 0.4-MPa strength in [12]. The maximum displacement of the supports before fracturing can also be compared. It is computed as the contact time multiplied by the speed of the supports: $\Delta x = v\Delta t = 0.1 \text{ m/s} \times 0.042 \text{ s} = 4.2 \text{ mm}$; after renormalization to 0.4-MPa strength, it coincides with the average value of 1.2 mm from [12] with 27% accuracy. The error in the computations can be fully explained by the heterogeneity of real ice, which is not taken into account in the numerical experiment.

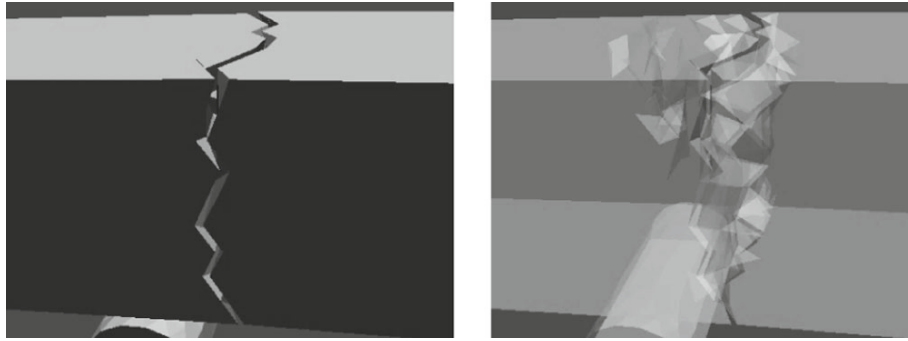


Fig. 10. External and internal structures of crack.

6. CONCLUSIONS

The experimental results presented in this paper demonstrate that our mechanical-mathematical model of ice adequately describes the real physical processes of ice fracturing, and they also show that its design parameters are consistent with the real ones. For further improvement of the ice behavior model, we need to take into account the dependence of the parameters on the deformation rate, which can be obtained based on the experimental data [13].

ACKNOWLEDGMENTS

This work was supported by the Russian Science Foundation, project no. 14-11-00434.

REFERENCES

1. SNIP (Building Regulations) No. 2.06.04-82*, Loads and impacts on hydraulic structures (wave, ice and ships) (2012).
2. Rules of the Russian Maritime Register of Shipping PBU/MSP (2014).
3. D. Hilding, J. Forsberg, and A. Gurtner, "Simulation of loads from drifting ice sheets on offshore structures," in *Proceedings of the 12th International LS-DYNA Users Conference*.
4. D. Hilding, J. Forsberg, and A. Gurtner, "Simulation of ice action loads on offshore structures," in *Proceedings of the 8th European LS-DYNA Users Conference, Strasbourg, 2011*.
5. B. Sand and L. Fransson, "Numerical simulation of level ice loads on Norstromsgrund lighthouse," in *Proceedings of the International Conference on Cold Climate Technology, Norway, 2014*.
6. Z. Liu, J. Amdahl, and S. Loset, "Plasticity based material modelling of ice and its application to ship-iceberg impacts," *Cold Reg. Sci. Technol.* **65**, 326–334 (2011).
7. Y. Gao, Zh.-q. Hu, J. W. Ringsberg, and J. Wang, "An elastic-plastic ice material model for ship-iceberg collision simulations," *Ocean Eng.* **102**, 27–39 (2015).
8. V. D. Ivanov, V. I. Kondaurov, I. B. Petrov, and A. S. Kholodov, "Calculation of dynamic deformation and disstructure of elastic-plastic body by grid-characteristic methods," *Mat. Model.* **2** (11), 10–29 (1990).
9. V. A. Lobanov, "Ice modeling in problems with finite element setting," *Differ. Uravn. Protsessy Upravl.*, No. 4, 19–29 (2008).
10. V. A. Miryaha, A. V. Sannikov, and I. B. Petrov, "Discontinuous Galerkin method for numerical simulation of dynamic processes in solids," *Math. Models Comput. Simul.* **7**, 446–455 (2015). doi: 10.1134/S2070048215050087
11. R. Radovitzky, A. Seagraves, M. Tupek, and L. Noels, "A scalable 3D fracture and fragmentation algorithm based on a hybrid, discontinuous Galerkin, cohesive element method," *Comp. Methods Appl. Mech. Eng.* **200**, 326–344 (2011).
12. S. Ehlers and P. Kujala, "Optimization-based material parameter identification for the numerical simulation of sea ice in four-point bending," *Proc. Inst. Mech. Eng., Part M: J. Eng. Maritime Environ.* **228**, 70–80 (2014).
13. A. T. Bekker, *Probability Characteristics of Ice Loads on Structures of the Continental Shelf* (Dalnauka, Vladivostok, 2004) [in Russian].

Translated by Yu. Kornienko